JOURNAL OF SOLID STATE CHEMISTRY 76, 33–39 (1988)

Crystal Structure and Magnetic Properties of Linear Chain Potassium Aquotetrafluoromanganate(III)

FERNANDO PALACIO* AND MERCEDES ANDRES

Instituto de Ciencia de Materiales de Aragón, CSIC, Universidad de Zaragoza, Facultad de Ciencias, 50009 Zaragoza, Spain

AND C. ESTEBAN-CALDERON, M. MARTINEZ-RIPOLL, AND S. GARCIA-BLANCO

Departmento de Rayos X, Institución Rocasolano, CSIC, Serrano 119, 28006 Madrid, Spain

Received December 2, 1987; in revised form March 7, 1988

The crystal structure and single-crystal ac magnetic susceptibilities of $KMnF_4 \cdot H_2O$ are reported. The structure, which is isomorphous to that of $RbMnF_4 \cdot H_2O$, consists of chains of alternating *trans*-$[MnF_4F_{2/2}]^{2-}$ and *trans*-$[MnF_2F_{2/2}(H_2O)_2]$ tetragonally elongated octahedra connected to each other by shared apical fluorine atoms. Crystal data: Space group $C2/c$, $a = 13.907(1)$ Å, $b = 6.2136(2)$ Å, $c = 10.492(1)$ Å, $\beta = 104.69(1)°$, $V = 877.0(2)$ Å^3, $D_c = 2.85$ g cm^{-3}, $Z = 8$, $R = 0.044$. Magnetic susceptibility measurements show a broad maximum around 52 K indicative of lower dimensionality behavior. The data may be fit to a Heisenberg $S = 2$ linear chain model with $J/k_B = -6.5$ K and $g = 2.05$. At 8.45 K a sharp peak in the susceptibility data parallel to the chains indicates weak ferromagnetic behavior.

Introduction

The search for and study of materials with quasi-one-dimensional magnetic properties is a long-standing area of active research (see, for example, (*1*)). Fluorinated Mn(III) compounds provide a number of such materials with potentially interesting properties, since the influence of a strong Jahn–Teller effect (*2*) favors a tendency to form chains or layers of corner-sharing coordination octahedra. Thus, the crystalline structure of $(NH_4)_2MnF_5$ consists of chains of *trans*-$[MnF_4F_{2/2}]^{2-}$ octahedra (*3*) while similar types of chains appear in $A^I_2MnF_5 \cdot H_2O$, with A^I = K (*4*), Rb (*5*, *6*), and Cs (*7*), and in $A^{II}MnF_5 \cdot H_2O$, with A^{II} = Sr and Ba (*8*). The H_2O molecules lie between the chains. It is worth noting however that, as a general rule, monohydrated salts with formula $A_2MX_5 \cdot H_2O$, where M is a trivalent transition metal and X is a halogen ion, tend to consist of discrete $[MX_5(H_2O)]^{2-}$ units. That is the case, for example, for $K_2CrF_5 \cdot H_2O$ (*9*), $A_2FeX_5 \cdot H_2O$ (A = K, NH_4, Rb, Cs; X = F, Cl, Br) (*10*), or $(NH_4)_2MoX_5 \cdot H_2O$ (X = Cl, Br) (*11*). One of the few exceptions to this rule is the hydrothermally prepared β-$Rb_2FeF_5 \cdot H_2O$ which also exhibits *trans*-linked $[FeF_4F_{2/2}]^{2-}$ chains (*12*).

On the other hand, when the number of fluorine atoms per formula unit is four,

* To whom correspondence should be addressed.

0022-4596/88 $3.00

Mn(III) compounds do not seem to present such homogeneous behavior. In fact, the crystalline structure of tetrafluoromanganate(III) derivatives can be formed by layers, chains, or isolated coordination octahedra, depending on the number of water molecules in the formula unit. Thus, $CsMnF_4$ is known to form layers of elongated *trans*-$[MnF_2F_{4/2}]^-$ octahedra, where the four fluorine atoms placed at the layer plane are shared by four neighbor octahedra, its structure being of the $TlAlF_4$ type (*13*). The compound $RbMnF_4 \cdot H_2O$ consists of chains in which alternate *trans*-$[MnF_4F_{2/2}]^{2-}$ and *trans*-$[MnF_2F_{2/2}(H_2O)_2]$ octahedra are connected with each other by sharing apical fluorine atoms (*14*). Finally, compounds with two molecules of water in the formula, such as $CsMnF_4 \cdot 2H_2O$ (*15*) and $(CH_3)_4NMnF_4 \cdot 2H_2O$ (*14*) have a structure formed by isolated $[MnF_4(H_2O)_2]^-$ octahedra. Under this scheme, $KMnF_4 \cdot H_2O$ should exhibit a coordinative behavior similar to $RbMnF_4 \cdot H_2O$ and, therefore, present one-dimensional properties.

A further reason of interest in the present study is that Mn(III) is, together with Cr(II), a d^4 ion. Little is known of the magnetic properties of compounds of d^4 ions generally, and less is known about the magnetic properties of Mn(III) derivatives. In a recent paper we have reported on the magnetic properties of $RbMnF_4 \cdot H_2O$ (*16*) showing that, apart from its one-dimensional antiferromagnetic behavior, it exhibits at the (3-d) ordering temperature a canting between both magnetic sublattices. It is as well relevant to verify whether weak ferromagnetic properties are also present in the potassium derivative. In this paper we present the crystalline structure and magnetic properties of $KMnF_4 \cdot H_2O$ and compare them with those of the Rb analog.

Experimental Section

A. Sample preparation. Manganese(III) oxide, prepared by heating MnO_2 at 700°C (*17*), was dissolved in 20% hydrofluoric acid and the MnF_3 formed was allowed to diffuse into a hydrofluoric acid solution of KF. The MnO_2 : KF molar ratio used was always somewhat higher than 1 : 1 because the reduction of MnO_2 to Mn_2O_3 was never quantitative. A gel made with 2% of agar–agar was used as support for the diffusion process (*18*). After a few days, two distinct specimens of crystals, which from chemical analysis were shown to be $KMnF_4 \cdot H_2O$ and $K_2MnF_5 \cdot H_2O$, could be collected from the intermediate gel phase and readily separated from each other because of their different color and shape. $KMnF_4 \cdot H_2O$ was recrystallized by slow evaporation of a solution of the appropriate crystals in 2 *N* hydrofluoric acid. (Found: Mn, 29.33%; calc: Mn, 29.23%.)

Large single crystals, of about 15 mg, suitable for susceptibility measurements were obtained after 2 to 3 months of slow evaporation of saturated solutions of $KMnF_4 \cdot H_2O$ in 2 *N* hydrofluoric acid. The external morphology of these crystals tends to be prismatic with a rhombic cross section, the prism axis being parallel to the [100] direction of the crystal while the small diagonal of the rhombic section lies parallel to the [010] direction.

B. Magnetic measurements. Magnetic ac susceptibility measurements, at zero external magnetic field, were made between 4.2 and 100 K on single crystals along directions parallel to the three principal axes of the susceptibility tensor. The frequency of the excitation current was 333 Hz, the alternating field at the coils being 10^{-4} T.

Correction for diamagnetic contribution of the molecule falls within the experimental error and was not taken into account. The effect of temperature-independent paramagnetism (TIP) was more difficult to calculate since at 100 K short-range interactions, typical of the lower dimensionality characteristics of the compound, were not

negligible. Nevertheless, from the asymptotic behavior of the experimental data one can estimate that TIP affects the experimental points for, at the most, 5%, which in turn does not have an influence on the fitted values of J_B/k and g.

C. Crystal data and structure analysis. All measurements on a brown-colored single crystal of 0.37 × 0.30 × 0.30 mm were made on a fully automated diffractometer with graphite-monochromated Mo$K\alpha$ radiation (λ = 0.71069 Å). The cell parameters were determined by least-squares fit from the Bragg angles for 35 reflections measured for both positive and negative 2θ angles. Intensities of 2009 independent reflections were collected up to θ = 40° with an $\omega/2\theta$ scan technique. No crystal decomposition was observed. An absorption correction was performed using the ORABS (*19*) program. One thousand twenty one reflections were considered as observed with $I > 2\sigma(I)$ and used in the remaining calculations. Lorentz and polarization effects were applied as usual (Table I).

Atomic positions taken from the isomorphous Rb compound (*14*) were used to start with the least-squares refinements. A difference synthesis, calculated with those reflections with $\sin\theta/\lambda < 0.5$ Å^{-1}, clearly showed both H atoms of the water molecule. To prevent bias on $\langle w\Delta^2F\rangle$ vs $\langle F_o\rangle$ and vs $\langle \sin\theta/\lambda\rangle$, the last steps of the refinement were carried out with weights given by $w = w_1 \cdot w_2$, where $w_1 = 1/(a + b\,|F_o|)^2$ and $w_2 = 1/(c + d \sin\theta/\lambda)$ with coefficients shown in Table II. Final refinement, including positional parameters of the H atoms, led to R = 0.044 and R_w = 0.051.[1]

TABLE I

CRYSTAL DATA

Molecular formula	H_2F_4MnOK
Formula weight	188.05
Crystal system	Monoclinic
Space group	$C2/c$
a	13.907(1) Å
b	6.2136(2) Å
c	10.492(1) Å
β	104.69(1)°
V	877.0(2) Å^3
D_c	2.85 g cm^{-3}
Z	8
$F(000)$	720
λ	0.71069 Å
μ	38.27 cm^{-1}

TABLE II

COEFFICIENTS FOR THE WEIGHTING SCHEME

	a	b		c	d
$F_o \le 9$	1.32	−0.05	$\sin\theta/\lambda \le 0.57$	3.60	−5.57
$F_o > 9$	0.27	0.04	$0.57 < \sin\theta/\lambda \le 0.69$	−1.63	3.69
			$\sin\theta/\lambda > 0.69$	0.40	0.66

Results and Discussion

Final positional and thermal parameters for the compound are given in Table III. A half-normal probability plot (*21*) comparing our fractional coordinates with the ones given for the isomorphous Rb derivative (*14*) gives a linear array with a correlation coefficient of 0.98 (Rb and K have been excluded).

Table IV contains a list of bond lengths and bond angles and a projection of the structure down the b axis is shown in Fig. 1. The geometry around the Mn octahedra is in good agreement with the one found for the Rb compound (*14*). Similarly, the elongation of some of the Mn–O and Mn–F distances is to be ascribed mainly to the Jahn–Teller effect.

The H atoms of the water molecule are involved in two hydrogen bonds (Table III). One of them, O(1)...F(3)^{II}, connects two parallel chains of Mn octahedra and shows a typical geometry. The other H bond (in-

[1] Most calculations were performed using the X-RAY 70 system (*20*) on the UNIVAC 1100/80 computer, J.E.N., Madrid.

TABLE III

ATOMIC COORDINATES AND THERMAL PARAMETERS AS $U_{eq} = \frac{1}{3} \Sigma_i \Sigma_j U_{ij} a_i^* a_j^* (a_i \cdot a_j)$

	x/a	y/b	z/c	U_{eq} (×10⁴)
K	0.0806(0)	0.7422(1)	0.4425(1)	300(2)
Mn(1)	0.2500(0)	0.2500(0)	0.5000(0)	137(1)
Mn(2)	0.0000(0)	0.2469(1)	0.2500(0)	132(1)
F(1)	0.1075(1)	0.2539(3)	0.4368(2)	264(5)
F(2)	0.2501(1)	−0.0317(2)	0.4621(2)	282(5)
F(3)	0.0649(1)	0.0349(3)	0.1817(2)	349(5)
F(4)	0.0681(1)	0.4569(3)	0.1863(2)	308(5)
O(1)	0.2644(1)	0.3249(3)	0.3052(2)	270(6)
H(1)	0.320(8)	0.414(16)	0.314(9)	630(0)
H(2)	0.220(7)	0.394(16)	0.266(9)	630(0)

ter- and intrachain) could be accepted as asymmetrically bifurcated.

Magnetic susceptibility measurements are shown in Fig. 2. The axes labeled as *d* and *e* correspond to directions parallel and perpendicular to the chain within the *ac* plane, respectively. Two of the principal axes of the susceptibility tensor must lie in the *ac* plane, and correspond to directions of maximum and minimum susceptibility. The data indicate that the *e* axis is in fact the axis of preferred antiferromagnetic alignment because the susceptibility tends to zero value at low temperatures. The *b* axis, which is necessarily a principal axis of the susceptibility tensor for a monoclinic system, is a hard perpendicular axis of an ordered antiferromagnet, for it maintains a constant value after it rises to a maximum of the susceptibility.

At temperatures above 10 K, there appears a broad maximum at about 52 K corresponding to the one-dimensional character of the compound. The maximum, which is clearly observed along the *e* and *d* axes, is hardly detected along the *b* axis where it appears to be around 38 K.

Below 10 K the data observed parallel to the *d* axis exhibit a very sharp peak at about 8.45 K. The small peaks observed in the data parallel to the *b* and *e* directions are due to minor misorientations of the crystal. A similar behavior has also been observed in the case of $RbMnF_4 \cdot H_2O$ (*16*), although in the present case the peak is sharp and does not exhibit the satellite peaks which appear in the Rb compound. The behavior is characteristic of a 1-d antiferromagnetic alignment with the magnetic moments canted toward the *d* axis within the *ac* crystallographic plane. As a consequence a weak ferromagnetic moment below the ordering temperature is present.

The fit from high-temperature series (hts) expansion for a Heisenberg $S = 2$ linear chain (*22*) together with the values for

TABLE IV

BOND LENGTHS (Å) AND ANGLES (°)

Distances and angles of Mn(1) octahedron			
Mn(1)–F(1)	1.924(1)	F(1)–Mn(1)–F(2)	89.70(7)
Mn(1)–F(2)	1.795(1)	F(1)–Mn(1)–O(1)	90.33(7)
Mn(1)–O(1)	2.155(2)	F(2)–Mn(1)–O(1)	89.70(9)
Distances and angles of Mn(2) octahedron			
Mn(2)–F(1)	2.143(2)	F(1)–Mn(2)–F(3)	94.20(7)
Mn(2)–F(3)	1.842(2)	F(1)–Mn(2)–F(4)	90.79(7)
Mn(2)–F(4)	1.835(2)	F(1)–Mn(2)–F(3)^{I}	87.48(7)
		F(1)–Mn(2)–F(4)^{I}	87.55(7)
		F(3)–Mn(2)–F(4)	91.00(8)
		F(3)–Mn(2)–F(3)^{I}	88.69(9)
		F(4)–Mn(2)–F(4)^{I}	89.37(8)
		F(1)–Mn(2)–F(1)^{I}	177.66(7)
		F(3)–Mn(2)–F(4)^{I}	178.21(7)
Distances of K polyhedron			
K–F(1)	3.060(2)	K–F(1)^{IV}	3.182(2)
K–F(4)	3.188(2)	K–F(2)^{V}	2.658(2)
K–F(4)^{I}	2.798(2)	K–F(3)^{VI}	2.923(2)
K–F(1)^{III}	3.204(2)	K–F(3)^{VII}	2.786(2)
K–F(2)^{III}	2.707(2)	K–F(4)^{VI}	2.886(2)
K–F(3)^{III}	3.246(2)		

Intermolecular contacts

X–H...Y	X...Y (Å)	X–H (Å)	H...Y (Å)	<X–H...Y (°)
Intramolecular				
O(1)–H(2)...F(4)[a]	2.820(2)	0.77(9)	2.11(9)	153(10)
Intermolecular				
O(1)–H(1)...F(3)^{II}	2.681(3)	0.93(9)	1.76(9)	168(9)
O(1)–H(2)...F(2)^{II}[a]	2.900(3)	0.77(9)	2.57(9)	108(9)

Note. Symmetry operations: I, $-x, y, 0.5 - z$; II, $0.5 - x, 0.5 + y, 0.5 - z$; III, $x, 1 + y, z$; IV, $-x, 1 - y, 1 - z$; V, $0.5 - x, 0.5 - y, 1 - z$; VI, $x, 1 - y, 0.5 + z$; VIII, $-x, 1 + y, 0.5 - z$.

[a] Asymmetrically bifurcated hydrogen bond.

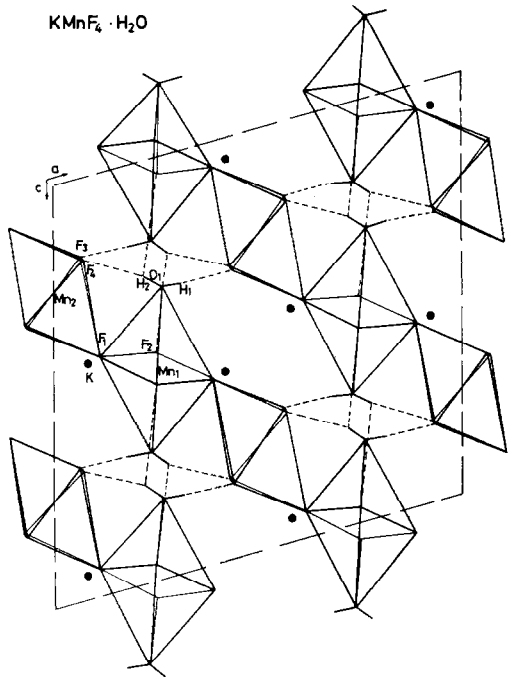

FIG. 1. Crystal structure of $KMnF_4 \cdot H_2O$ projected on the *ac* plane. Dotted lines indicate hydrogen bonds.

$k_B T_{max}/|J| = 6.78$ and $\chi_{max}|J|/Ng^2\mu_\beta^2 = 0.095$, calculated by Navarro from hts by extrapolation techniques (*23*), gives $J/k_B = -6.5$ K with $g = 2.05$.

These values are almost equal to the fitted values obtained in the case of the analogous $RbMnF_4 \cdot H_2O$ compound (*16*), where $J/k_B = -6.2$ K with $g = 2.03$. An explanation for such similar magnetic behavior can be found by comparing superexchange pathways through the chains in both compounds. Intrachain magnetic interactions extend through zigzag Mn–F–Mn bridges, the angles at the fluorine vertex being 137.2 and 138.0° for the K and Rb compounds, respectively, with in-chain Mn–Mn distances of 4.081 and 4.108 Å, respectively. According to the Goodenough and Kanamori rules (*24*) the intensity of the superexchange interaction should strongly depend on the Mn–F–Mn angle which is closely related with the overlap of σ-orbitals involved in the bridging bonds. Therefore, it is not surprising to find in $KMnF_4 \cdot H_2O$ a 1-d magnetic behavior very near to that found for $RbMnF_4 \cdot H_2O$.

It is more interesting to compare the magnetic and structural behavior of these compounds with other fluoromanganate(III) linear chain derivatives (*25*) by using the linear correlation found by Massa and Pebler (*26*). In Fig. 3, the intensity of the superexchange interaction is plotted as a function of the Mn–F–Mn angle for $KMnF_4 \cdot H_2O$ and $RbMnF_4 \cdot H_2O$ and compared with other previously reported Mn(III) derivatives. It is remarkable that these two linear chain compounds are the only ones in which oxygen atoms are involved in the coordination sphere of Mn(III) ions and yet only a small influence, mostly due to the

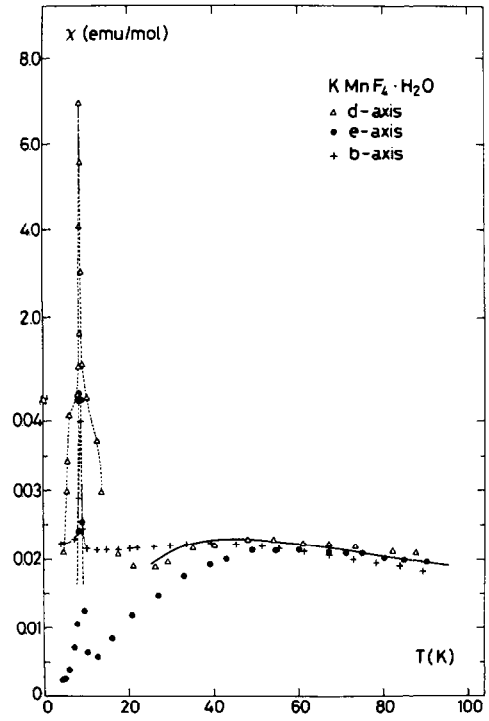

FIG. 2. Temperature dependence of zero-field magnetic susceptibility along the three principal axes. For $T < 10$ K a dotted line is used as guide to the eye. Solid line is the theoretical calculation (see text).

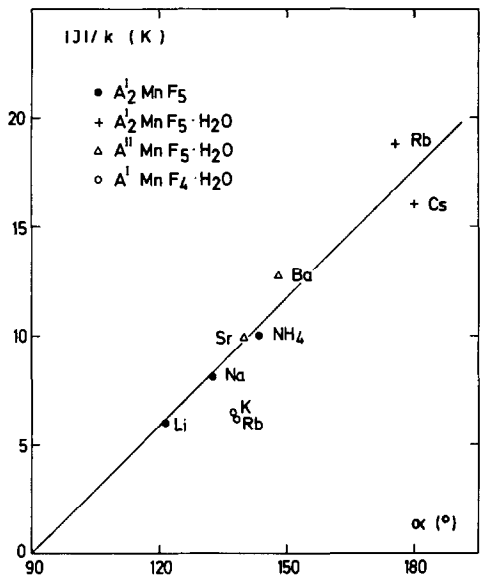

FIG. 3. Correlation between magnetic exchange interaction and pathway angle.

different Jahn–Teller distortion within the chains, can be detected on the magneto-structural correlations.

The chains in the magnetic system are not isolated from one another since at a temperature somewhat above 8.45 K three-dimensional interaction between chains establishes a transition to an ordered antiferromagnet with small canting in the magnetic sublattices. It is not easy to establish precisely the temperature T_c at which the transition to long-range ordering occurs and the peak at $T = 8.45$ K can be given only as a lower bound for the value of T_c. In most antiferromagnets T_c is determined by the maximum slope in $\chi_\parallel$ (see, for example, (*27*)). In $KMnF_4 \cdot H_2O$ the easy axis of antiferromagnetic alignment is parallel to the *e* axis; however, at the temperature of the peak the values of the susceptibility data parallel to the *d* axis are three orders of magnitude higher than those parallel to the *e* axis and, therefore, a minute misorientation of the crystal greatly influences the observed susceptibilities along *e*. On the other hand, the existence of canting leads to a weak ferromagnetic moment along the *d* axis indicated by peaks in both in-phase and out-of-phase (*28*) components of the ac susceptibility curve. In fact, nonzero values of the out-of-phase component of the susceptibility at zero external magnetic field are indicative of absorption effects due to the presence of net magnetic moments. However, zero-field absorption effects are present up to 9.1 K, a temperature which should be considered well above T_c. A similar behavior has also been found in the analogous $RbMnF_4 \cdot H_2O$ where very slow relaxation processes are present and susceptibility measurements have to be considered, at the measuring frequency, as adiabatic ones (*16*). A more elaborate study of the weak ferromagnetic properties including magnetization and frequency dependence is in progress.

Finally, it is of interest to comment upon the ideality of the magnetic chain in the K derivative and to compare it with that of the Rb analog. In a system of weakly coupled chains, the ordering temperature can be considered to be the temperature at which the thermal energy equals the interaction energy between correlated chain segments (*29, 30*):

$$k_B T_c/|J| = \xi(T_c)RS(S + 1),$$

where $\xi(T_c)$ is the correlation length within the chain, and $R = |J'/J|$ is the ratio of inter- to intrachain exchange. For the Heisenberg chain

$$\xi(T) = 2|J|S(S + 1)/k_B T$$

so that

$$k_B T_c/|J| = S(S + 1)(2R)^{1/2}.$$

The above relation provides a value of $R = 2.3 \times 10^{-2}$ for $KMnF_4 \cdot H_2O$ which is essentially equal to $R = 2.2 \times 10^{-2}$ calculated in the case of $RbMnF_4 \cdot H_2O$. Since a certain degree of anisotropy is always present in

Mn(III) systems, the above values should be considered as an upper bound for R.

In conclusion, the present study shows that $KMnF_4 \cdot H_2O$ is a 1-d magnetic system presenting weak ferromagnetism below the magnetic ordering temperature. It is structurally isomorphous with $RbMnF_4 \cdot H_2O$, and both compounds exhibit similar magnetic behavior. Nevertheless, the shape of the peak due to weak ferromagnetism in the K compound differs from that exhibited by the Rb analog, a fact which permits one to expect differences between the spin-lattice relaxation properties of both compounds.

Supplementary material available. A listing of anisotropic thermal parameters and structure factor amplitudes is available (15 pages).[2]

Acknowledgments

The authors thanks Professor R. L. Carlin for his comments and critical reading of the manuscript. This work was supported by Comisión Asesora de Investigación Científica y Técnica, Grant 3380/83.

References

1. C. P. LANDEE, *in* "Organic and Inorganic Low Dimensional Crystalline Materials" (P. Delhaes and M. Drillon, Eds.), NATO Adv. Res. Workshop, Plenum, New York (1987).
2. P. KÖHLER, W. MASSA, D. REINEN, B. HOFFMAN, AND R. HOPPE, *Z. Anorg. Allg. Chem.* **446,** 131 (1978).
3. D. R. SEARS AND J. L. HOARD, *J. Chem. Phys.* **50,** 1066 (1969).
4. A. J. EDWARDS, *J. Chem. Soc. A,* 2653 (1971).
5. P. BUKOVEC AND V. KAUCIC, *Acta Crystallogr. Sect. B* **34,** 3339 (1978).
6. J. R. GÜNTER, J. P. MATTHIEU, AND H. R. OSWALD, *Helv. Chim. Acta* **61,** 328 (1978).
7. V. KAUCIC AND P. BUKOVEC, *Acta Crystallogr. Sect. B* **34,** 3337 (1978).
8. W. MASSA AND V. BURK, *Z. Anorg. Allg. Chem.* **516,** 119 (1984).
9. P. BUKOVEC, B. OREL, AND J. SIFTAR, *Monatsh. Chem.* **105,** 1299 (1974).
10. R. L. CARLIN AND F. PALACIO, *Coord. Chem. Rev.* **65,** 141 (1985), and references therein.
11. R. G. CAVELL AND J. W. QUAIL, *Inorg. Chem.* **22,** 2597 (1983).
12. J. L. FOURQUET, R. DE PAPE, J. TEILLET, F. VARRET, AND G. C. PAPAEFTHYMION, *J. Magn. Magn. Mater.* **27,** 209 (1982).
13. W. MASSA AND M. STEINER, *J. Solid State Chem.* **32,** 137 (1980).
14. V. KAUCIC AND P. BUKOVEC, *J. Chem. Soc. Dalton Trans.,* 1512 (1979).
15. P. BUKOVEC AND V. KAUCIC, *J. Chem. Soc. Dalton Trans.,* 945 (1977).
16. F. PALACIO, M. ANDRÉS, R. HORNE, AND A. J. VAN DUYNEVELDT, *J. Magn. Magn. Mater.* **54–57,** 1487 (1986).
17. W. G. PALMER, "Experimental Inorganic Chemistry," Cambridge Univ. Press, London (1954).
18. H. K. HAENISCH, "Crystal Growth in Gels," Pennsylvania State Univ. Press, University Park/London (1970).
19. D. SCHWARZENBACH, ORABS Program, Technische Hochschule, University of Zurich (1972).
20. J. M. STEWART, F. A. KUNDELL, AND J. C. BALDWIN, "The X-Ray 70 System," Computer Sci. Center, University of Maryland, College Park, MD (1970).
21. S. C. ABRAHAMS AND E. T. KEVE, *Acta Crystallogr. Sect. A* **27,** 157 (1971).
22. G. S. RUSHBROOKE AND P. J. WOOD, *Mol. Phys.* **1,** 257 (1958).
23. R. NAVARRO, Thesis, University of Zaragoza (1976).
24. P. W. ANDERSON, *in* "Magnetism" (G. T. Rado and H. Suhl, Eds.), Academic Press, New York (1963).
25. P. NUÑEZ, J. DARRIET, P. BUKOVEC, A. TRESSAUD, AND P. HAGENMULLER, *Mater. Res. Bull.* **22,** 661 (1987).
26. W. MASSA AND J. PEBLER, *in* "Proceedings, IIIrd. European Conference on Solid State Chemistry," Regensburg (1986).
27. R. L. CARLIN, "Magnetochemistry," Springer-Verlag, Berlin (1986).
28. Data to be published.
29. J. VILLAIN AND J. LOVELUCK, *J. Phys. Lett.* **38,** L77 (1977).
30. G. MENNENGA, L. J. DE JONGH, W. J. HUISKAMP, AND J. REEDIJK, *J. Magn. Magn. Mater.* **44,** 89 (1984).

[2] See NAPS Document No. 04599 for 15 pages of supplementary materials from ASIS/NAPS, Microfiche Publications, P.O. Box 3513, Grand Central Station, New York, NY 10163. Remit in advance, in U.S. funds only, $7.75 for photocopies or $4.00 for microfiche. Outside the U.S. and Canada, add postage of $4.50 for the first 20 pages and $1.00 for each of 10 pages of material thereafter, or $1.50 for microfiche postage.